

# Methane storms as a driver of Titan's dune orientation

Benjamin Charnay<sup>1,2\*</sup>, Erika Barth<sup>3</sup>, Scot Rafkin<sup>3</sup>, Clément Nartreau<sup>4</sup>, Sébastien Lebonnois<sup>2</sup>, Sébastien Rodriguez<sup>5</sup>, Sylvain Courrech du Pont<sup>6</sup> and Antoine Lucas<sup>5</sup>

**The equatorial regions of Saturn's moon Titan are covered by linear dunes that propagate eastwards<sup>1-3</sup>. Global climate models (GCMs), however, predict westward mean surface winds at low latitudes on Titan, similar to the trade winds on Earth<sup>1,4</sup>. This apparent contradiction has been attributed to Saturn's gravitational tides<sup>1</sup>, large-scale topography<sup>4</sup> and wind statistics<sup>5</sup>, but none of these hypotheses fully explains the global eastward propagation of dunes in Titan's equatorial band. However, above altitudes of about 5 km, Titan's atmosphere is in eastward super-rotation, suggesting that this momentum may be delivered to the surface. Here we assess the influence of equatorial tropical methane storms—which develop at high altitudes during the equinox—on Titan's dune orientation, using mesoscale simulations of convective methane clouds<sup>6,7</sup> with a GCM wind profile that includes super-rotation<sup>8</sup>. We find that these storms produce fast eastward gust fronts above the surface that exceed the normal westward surface winds. These episodic gusts generated by tropical storms are expected to dominate aeolian transport, leading to eastward propagation of dunes. We therefore suggest a coupling between super-rotation, tropical methane storms and dune formation on Titan. This framework, applied to GCM predictions and analogies to some terrestrial dune fields, explains the linear shape, eastward propagation and poleward divergence of Titan's dunes, and implies an equatorial origin of dune sand.**

A major surprise in the exploration of Titan by Cassini was the discovery of large dune fields in the equatorial regions, which cover close to 15% of Titan's surface<sup>1-3</sup>. These giant dunes are linear and parallel to the equator, and are probably composed of hydrocarbon material. The analysis of dune morphology around obstacles and dune terminations indicates an eastward dune propagation with some regional variations<sup>1,2</sup> (see also Supplementary Fig. 1). However, GCMs predict that annual mean surface winds are easterlies (westward) at low latitudes<sup>4</sup>, as trade winds on Earth<sup>9</sup>. Therefore, Titan's dune orientation is opposite to predicted mean winds, raising a major enigma.

Given the nonlinear dependence of sediment transport on wind speed, the only way to propagate dunes eastwards would be the occurrence of episodic fast westerly (eastward) gusts<sup>5</sup>. Above 5 km, Titan's troposphere is in super-rotation with fast eastward winds at any latitude. Pumping momentum from this super-rotation down to the surface might provide a solution. However, Titan's tropospheric circulation is essentially confined into a 2 km boundary layer<sup>10</sup>.

Incidentally, this boundary layer circulation may explain the dune spacing of around 2 km (refs 10,11). Dry convection is therefore limited to the first 2 km and unable to reach the fast eastward winds<sup>10</sup>. The Köln GCM has been shown to generate episodic fast eastward gusts at the equator during Titan's equinoxes<sup>5</sup>. However, this result has not been reproduced by any published GCM, including the Titan IPSL GCM (used here), which faithfully reproduces the super-rotation and the thermal structure measured by the Huygens probe in the troposphere<sup>8,10</sup> in contrast to the Köln GCM. We therefore conclude that Titan's atmospheric general circulation is not likely to produce fast eastward winds at the equator.

Similar to the water cycle on Earth, Titan's weather is characterized by a methane cycle producing methane clouds. These clouds are rare over the equatorial region and probably absent during most of Titan's year<sup>12</sup>. However, during the equinox, the circulation leads to a methane convergence at the equator, sufficient to trigger deep convection<sup>13,14</sup>. Tropical convective clouds have been detected during the equinoctial season<sup>12,15-17</sup> with top altitude between 10 and 30 km (ref. 17). Huge storm systems covering a large part of the equatorial band have been observed, one of them associated with methane precipitation<sup>15,16</sup>. On Earth, storms frequently generate gust fronts above the surface. They occur when downdrafts, generally cooled by rain evaporation, reach the ground below the storm, producing cold surface currents, also called cold pools<sup>18</sup>. The gust front is the leading edge of the cold pool, and its propagation is mostly controlled by the direction of upper winds.

To investigate whether Titan's storms might lead to the production of such gusts with a preferential direction, we analysed their formation under the wind shear produced by Titan's super-rotation with a mesoscale regional model. We ran two-dimensional (2D; longitude–altitude) mesoscale simulations with the Titan Regional Atmospheric Scale Modeling System<sup>6,7</sup> (TRAMS). This model includes full cloud microphysics (see Supplementary Information) with condensation, melting, freezing and evaporation of methane cloud particles.

For the initial conditions, we used the temperature profile measured by Huygens<sup>19</sup> and a wind profile from the Titan IPSL GCM with no methane cycle<sup>8</sup>. Huygens' measurements indicated a methane humidity of 40% at the surface<sup>20</sup>. These conditions do not allow the development of convective clouds but were measured at the end of the southern summer. For our simulations at the equinoctial season, we used a methane profile with a surface humidity of ~50% or 60%, which is necessary to form convective

<sup>1</sup>Virtual Planetary Laboratory, University of Washington, Box 351580, Seattle, Washington 98195, USA. <sup>2</sup>Laboratoire de Météorologie Dynamique, IPSL/CNRS/UPMC, 75252 Paris, France. <sup>3</sup>Southwest Research Institute, Boulder, Colorado 80302, USA. <sup>4</sup>Institut de Physique du Globe de Paris, CNRS-UMR 7154, Sorbonne Paris Cité, Université Paris-Diderot, 75238 Paris, France. <sup>5</sup>Laboratoire Astrophysique, Instrumentation et Modélisation, CNRS-UMR 7158, Université Paris-Diderot, CEA-SACLAY, 91191 Gif sur Yvette, France. <sup>6</sup>Laboratoire de Matière et Systèmes Complexes, CNRS-UMR 7057, Sorbonne Paris Cité, Université Paris-Diderot, 75013 Paris, France. \*e-mail: benjamin.charnay@lmd.jussieu.fr

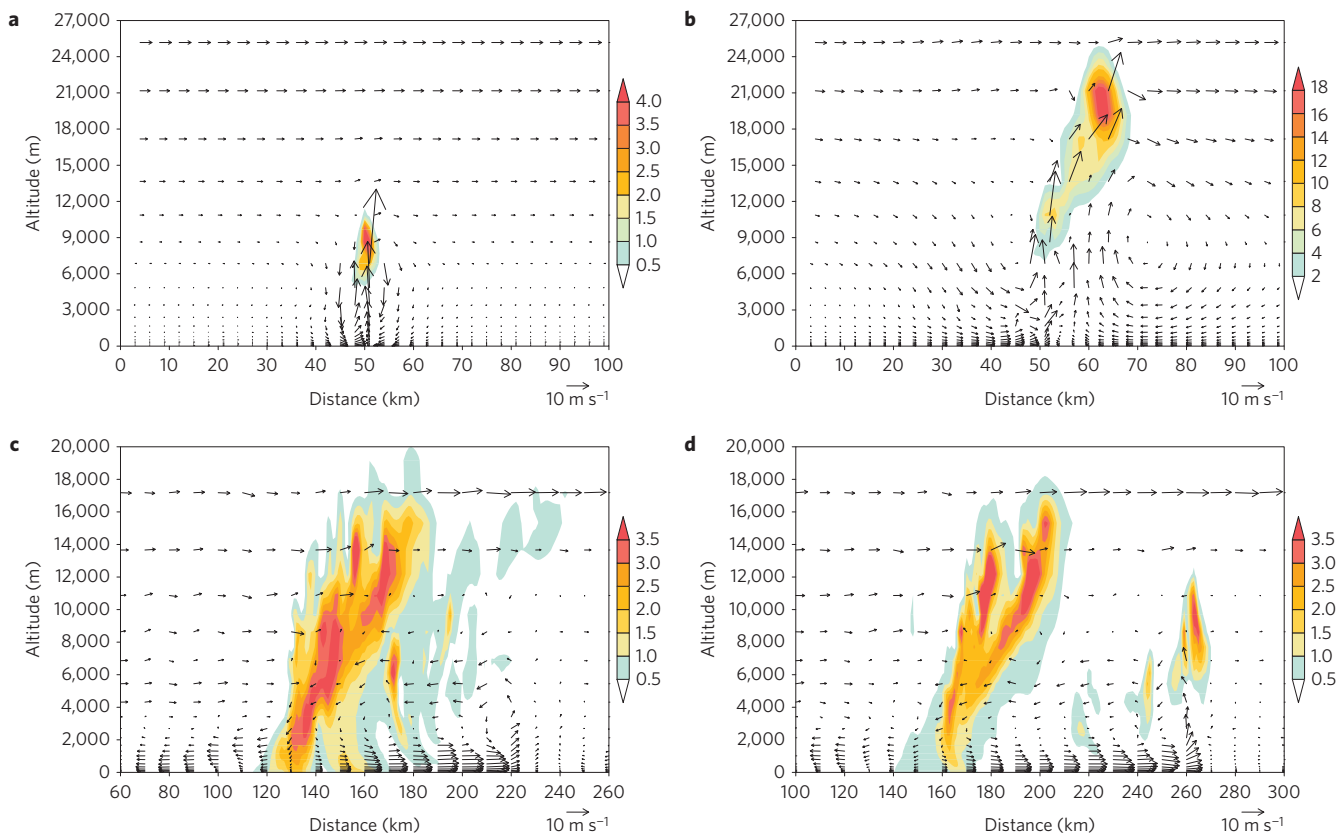


**Figure 1 | Two-dimensional (altitude–longitude) simulation of the evolution of a storm under Titan's conditions at the equator during equinox.**

**a–d**, Charts of the storm 1 h (**a**), 1 h 40 min (**b**), 10 h 35 min (**c**) and 12 h 30 min (**d**) after the start of the simulation. The initial wind profile was derived from the GCM. The initial methane humidity corresponds to a convective available potential energy of  $500 \text{ J kg}^{-1}$ . Colour bars indicate the mixing ratio of condensed methane in  $\text{g kg}^{-1}$ . The horizontal (vertical) component of wind vectors is scaled to the x axis (y axis). A reference vector of  $10 \text{ m s}^{-1}$  for zonal wind is shown. In **c** and **d**, the vertical wind component is reduced by 80% to better see the gust front.

clouds and corresponds to a convective available potential energy of 250 or  $500 \text{ J kg}^{-1}$ . The deep convection was triggered by a warm bubble of +2 K (that is, the air temperature is increased in the first kilometre). In our simulations, convective clouds reach an altitude of 25 km, where fast eastward winds flow, and the storm dynamics leads to the formation of an eastward gust front above the surface. Figure 1 shows the development of a gust front in one of our simulations. The triggering of the convection is associated with symmetric convergence of air below the cloud (Fig. 1a). The cloud develops obliquely because of the wind shear (Fig. 1b). To compensate for the ascending air in the storm, a downdraft forms behind the storm (Fig. 1b). Passing below the cloud, it is cooled by rain evaporation, which accelerates it, and flows at the surface, producing the gust front. Subsequently, the gust front ends up beyond the cloud (Fig. 1c). It raises surrounding air from the surface to 3–4 km, producing secondary convective clouds that can increase its energy and lifetime (Fig. 1d). The passage of the gust front also produces a local peak of eastward surface wind (Fig. 2a), travelling over large distances (in the order of 500 km in our simulations). Behind the gust front, wind speeds are typically one order of magnitude higher than usual winds close to the surface, and can reach  $10 \text{ m s}^{-1}$  during up to 9 h (Fig. 2a,b).

Our 2D simulations are representative of large storms or mesoscale convective systems. Individual small storms (for example, less than 30 km in diameter) should produce weaker and more isotropic gusts than in our simulations. Yet, multiple small storms should interact with each other and organize the convection to form large storm or mesoscale convective systems, as the giant cloud systems observed in September and October 2010 (ref. 15),

producing strong gust fronts with an eastward propagation. The dynamics of such large storms should be essentially 2D and qualitatively well represented by our idealized 2D simulations (see Supplementary Information). We estimate that each region of the equator might statistically undergo on the order of one gust front every equinox (that is, two per Titan year; see Supplementary Information).

The nature of the sand on Titan is not well known. The optimum grain size for saltation is estimated to be around  $300 \mu\text{m}$  with a threshold friction speed around  $0.04 \text{ m s}^{-1}$  (ref. 21), corresponding to a wind speed around  $0.9 \text{ m s}^{-1}$  at 35 m above the surface (see Supplementary Information). In our GCM, winds at 35 m and at the equator are generally below  $0.5 \text{ m s}^{-1}$  and do not exceed  $1 \text{ m s}^{-1}$  (see Supplementary Figs 2 and 3). Thus, usual winds on Titan are likely to generate only limited sand transport. Our GCM winds follow a Weibull distribution. They exceed the threshold friction speed of  $0.04 \text{ m s}^{-1}$  only 0.06% of the time, producing a westward sand flux at the equator of only  $0.0015 \text{ m}^2 \text{ yr}^{-1}$  (see Supplementary Information for the sand flux calculation). However, GCMs tend to underestimate sand flux as they miss local gusts<sup>22</sup>. To compensate for this, we also consider a 10 times stronger westward sand transport ( $0.018 \text{ m}^2 \text{ yr}^{-1}$ ) by increasing GCM wind speed by 20%. Storm gusts largely exceed the wind threshold by an order of magnitude. According to our mesoscale simulations, the sand flux produced by storms is 2.7 times stronger eastward than westward, and one storm per equinox (that is, two per Titan year) produces on average an eastward sand flux around  $0.15 \text{ m}^2 \text{ yr}^{-1}$ . Although episodic, tropical storms should therefore dominate the sand transport. A higher saltation threshold friction speed (for example,  $0.052 \text{ m s}^{-1}$ ; ref. 23)

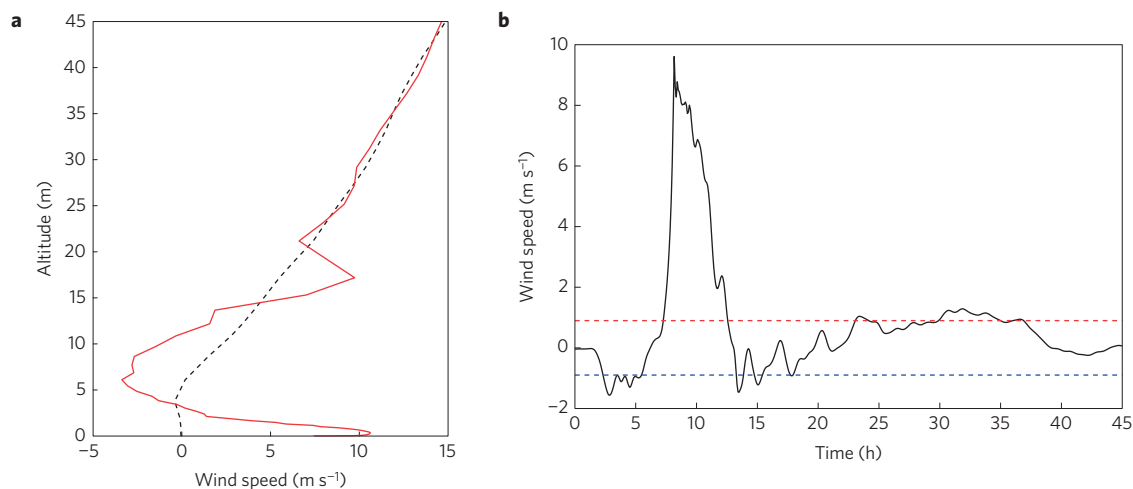


**Figure 2 | Wind speed in the gust front.** **a**, Wind profiles in the gust front (red) and without storm (black dashed line). **b**, Evolution of the zonal wind at 40 m (black line) during the passage of a gust front. Eastward winds are positive. The red (blue) dashed line corresponds to the threshold friction speed of  $0.04 \text{ m s}^{-1}$ , that is,  $0.9 \text{ m s}^{-1}$  at 40 m, for eastward (westward) winds.

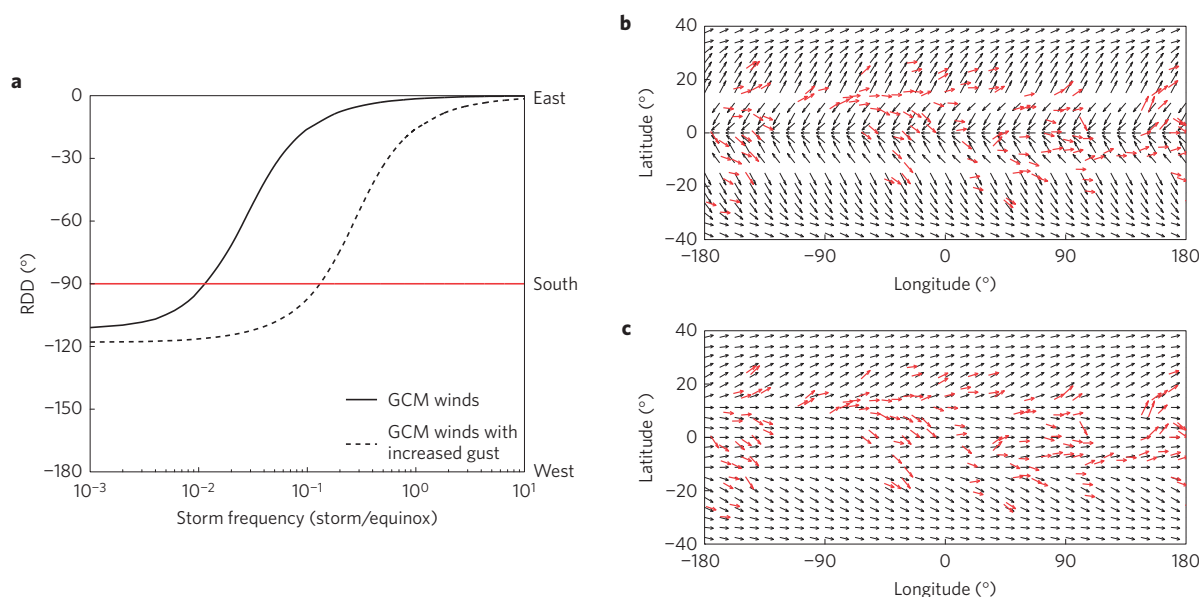


**Figure 3 | Storm impact on the RDD.** **a**, The RDD as a function of the storm frequency per equinox with a saltation threshold of  $0.04 \text{ m s}^{-1}$ , using GCM winds (black solid line) or GCM winds with increased gust (black dashed line). Angles are measured anticlockwise from the east (that is,  $-180^\circ$  is westward,  $-90^\circ$  is southward and  $0^\circ$  is eastward). The red line symbolizes the passage from westward to eastward dune growth. **b**, Map of dune orientation observed with Cassini's radar<sup>29</sup> (red) and map of RDD obtained with the GCM (with increased gust) for low latitudes with a threshold of  $0.04 \text{ m s}^{-1}$  and no storm effect (black). **c**, The same as **b**, but with the impact of two storms per Titan year.

would strongly reduce the sand flux from general circulation winds, but would weakly impact sand transport by storm gusts.

On Earth, although in unlimited sediment many linear dunes are oriented orthogonally to the direction of maximum sediment transport<sup>24</sup>, in limited sediment they align with the resultant transport direction, called the resultant drift direction (RDD), and propagate over long distances with regular spacing and a limited amount of sediment in interdune areas<sup>25</sup>. This mechanism may explain the formation and the evolution of Titan's dune fields. It requires neither cohesion<sup>26</sup> nor complex secondary flows, but relies on the presence of sedimentary reservoirs and multidirectional wind regimes producing an overall sediment flux over a non-erodible ground<sup>25</sup>. Given that many locations in Titan's dune fields seem to have sand-free bedrock interdunes<sup>3</sup>, the conditions of linear dune down-axis extension seem to be met.

Figure 3a shows the RDD combining winds from the Titan IPSL GCM with no topography and storm gusts from mesoscale simulations, with respect to the storm frequency. With no storm or a very small frequency of storm, the RDD is oriented westward with a southward component due to Saturn's eccentricity, which leads to stronger solar forcing and increased Hadley circulation during the southern summer (hence producing southward winds stronger than northward winds during the northern summer). With around two storm per Titan year (that is, one per equinox), the sand transport produced by equinoctial storms dominates and the RDD is oriented eastward. With such a frequency, the storm control remains efficient even for the GCM winds with increased gust.

For a 100-m-high dune, the eastward sand flux produced by two storms per Titan year (that is,  $0.15 \text{ m}^2 \text{ yr}^{-1}$ ) corresponds to an extension rate of  $3 \text{ mm yr}^{-1}$  (see Supplementary Information).

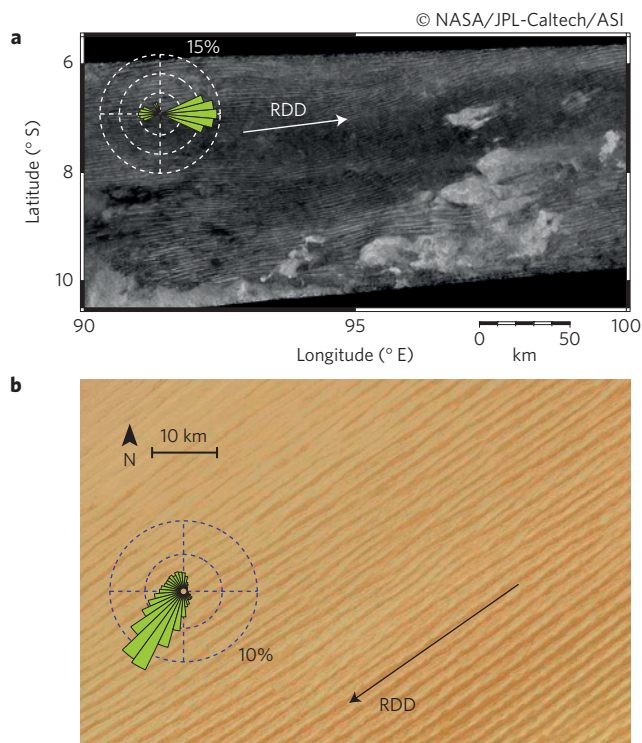


**Figure 4 | Analogy between linear dunes on Titan and in Rub'al-Kali desert on Earth.** **a**, Denoised image of Titan's dunes from Cassini's radar SAR, flyby T8 (see Supplementary Information). The inset shows the sand flux rose calculated at 7.5° S and averaging the effect of Saturn's eccentricity. **b**, Longitudinal dunes in Rub'al-Kali desert (Map data: Google; 18° N, 48° E) with the sand flux roses showing the distribution (in percentage) of sand flux as a function of the direction and calculated from winds at 10 m. For both images, the arrow corresponds to the RDD calculated with the sand flux rose.

According to the typical length of Titan's dunes (that is, 30–50 km; ref. 27), this implies a minimum formation time of around 15 Myr. This time is longer than the period of Saturn's perihelion precession (that is, 45 kyr), which corresponds to the switch of the warmest summer between both hemispheres. Thus, the southward component due to this orbital effect should vanish in dune orientation. Barchans and small dunes have been observed with shifted orientation as compared with long dunes<sup>28</sup>. This has been interpreted as the effect of a long-term, cyclic multimodal wind regime. Small dunes may indeed respond to long orbital changes (affecting both general circulation winds and storm impact), but our multimodal wind pattern can also explain their shifted orientation by growth orthogonal to the direction of maximum sediment transport<sup>24,25</sup>. Figure 3b,c shows the RDD map in the equatorial band without or with the effect of two storms per Titan year. In both cases, we averaged the effect of Saturn's eccentricity according to the above discussion. Our GCM predicts a RDD slightly converging to the equator for latitudes lower than 12° N/S and diverging from the equator for latitudes higher than 12° N/S. The divergence is due to faster poleward summer winds. This may explain the observed poleward orientation of dunes for latitudes higher than around 10° N/S (refs 2,29). These poleward sand fluxes also imply that Titan's sand cannot be transported from polar regions to the equatorial band. The sand of Titan's dunes must therefore have been produced in equatorial regions.

The sand flux pattern that we estimate for Titan's dunes is similar to those implicated in the formation of longitudinal dunes in the Rub'al-Kali desert (southern Arabia) and in the

Great Sand Sea (Egypt). In these deserts subject to a dominant wind, linear dunes are parallel to the RDD (see Fig. 4b and Supplementary Fig. 6). We can therefore establish an analogy with Titan's dune formation (Fig. 4). In terrestrial deserts, gust fronts formed by convective clouds can produce dust storms, also called haboobs<sup>30</sup>. Similarly, gust fronts generated by Titan's storms could produce dust storms. Indeed, their friction speed might exceed the threshold for micrometric particles (around  $4 \text{ m s}^{-1}$  at 35 m for a 10- $\mu\text{m}$ -diameter particles, see Supplementary Information). They could also transport centimetric pebbles (threshold speed around  $4\text{--}9 \text{ m s}^{-1}$  at 35 m for 1–5-cm-diameter pebbles), explaining the diffuse material trailing out to the east around many mountains<sup>27</sup>.

In conclusion, the combination of GCM and mesoscale simulations, together with analogies with terrestrial dune formation, provides a comprehensive scheme to explain the main features of Titan's dunes (that is, eastward propagation, linear shape, poleward divergence and 2–3 km spacing). This analysis highlights the potential importance of storms and mesoscale phenomena on aeolian processes. Such rare and strong events may play or have played an important role in some dune fields on Earth and Mars.

## Methods

Our analysis was performed using GCM and mesoscale simulations, together with analogies with terrestrial dunes. We use the Titan IPSL GCM (refs 8,10) to predict surface winds in the equatorial regions. This GCM reproduces well the super-rotation and the thermal structure measured by the Huygens probe in the troposphere. Simulations are performed taking into account the effects of the diurnal cycle and Saturn's gravitational tides, but with no topography and no methane cycle (see also Supplementary Information). Titan's climate is essentially dry, except in polar regions. The methane cycle is therefore not expected to significantly affect the tropospheric dynamics in the equatorial regions. This is illustrated by the excellent match between the thermal structure and its different layers measured by the Huygens probe and simulated by the GCM (ref. 10). To compute wind statistics and sand transport, we use instantaneous GCM surface winds over a year and all longitudes.

Methane storms are simulated with the mesoscale model TRAMS in two dimensions including full methane cloud microphysics (see also Supplementary Information)<sup>6,7</sup>. Incidentally, a GCM including the methane cycle cannot resolve storm cold pools and gust fronts, which are subgrid phenomena. As boundary conditions, we use the GCM zonal wind profile at the equator and at the north spring equinox, the Huygens temperature profile<sup>19</sup> and the Huygens methane humidity profile with an increase in the lower troposphere. These idealized simulations are representative of large or squall line storms. We estimate the order of magnitude of the storm frequency at each location in the equatorial band around one storm every equinox. A simple estimation of the size and displacement of the giant arrow-shape storm observed by Cassini at the equinox in 2009 (refs 15,16) gives a lower limit of 0.2 storm per equinox (see Supplementary Information). To compute the sand transport and sand flux roses produced by general circulation winds and gust fronts, we use a sand flux formula with a saltation threshold speed estimated from previous studies<sup>21</sup>. We also establish an analogy between Titan's dunes and some terrestrial dune fields, in particular in southern Arabia and Egypt (see Fig. 4 and Supplementary Fig. 6), where we predict sand fluxes from wind reanalysis data. The simulation data are available from B.C. on request.

Received 9 December 2014; accepted 6 March 2015;  
published online 13 April 2015

## References

- Lorenz, R. D. *et al.* The sand seas of Titan: Cassini RADAR observations of longitudinal dunes. *Science* **312**, 724–727 (2006).
- Lorenz, R. D. & Radebaugh, J. Global pattern of Titan's dunes: Radar survey from the Cassini prime mission. *Geophys. Res. Lett.* **36**, L03202 (2009).
- Rodríguez, S. *et al.* Global mapping and characterization of Titan's dune fields with Cassini: Correlation between RADAR and VIMS observations. *Icarus* **230**, 168–179 (2014).
- Tokano, T. Dune-forming winds on Titan and the influence of topography. *Icarus* **194**, 243–262 (2008).
- Tokano, T. Relevance of fast westerlies at equinox for eastward elongation of Titan's dunes. *Aeolian Res.* **2**, 113–127 (2010).
- Barth, E. L. & Rafkin, S. C. R. TRAMS: A new dynamic cloud model for Titan's methane clouds. *Geophys. Res. Lett.* **34**, L03203 (2007).

7. Barth, E. L. & Rafkin, S. C. R. Convective cloud heights as a diagnostic for methane environment on Titan. *Icarus* **206**, 467–484 (2010).
8. Lebonnois, S., Burgalat, J., Rannou, P. & Charnay, B. Titan global climate model: A new 3-dimensional version of the IPSL Titan GCM. *Icarus* **218**, 707–722 (2012).
9. Zhu, X., Strobel, D. F. & Flasar, M. F. Exchange of global mean angular momentum between an atmosphere and its underlying planet. *Planet. Space Sci.* **56**, 1524–1531 (2008).
10. Charnay, B. & Lebonnois, S. Two boundary layers in Titan's lower troposphere inferred from a climate model. *Nature Geosci.* **5**, 106–109 (2012).
11. Lorenz, R. D., Claudin, P., Andreotti, B., Radebaugh, J. & Tokano, T. A 3 km atmospheric boundary layer on Titan indicated by dune spacing and Huygens data. *Icarus* **205**, 719–721 (2010).
12. Rodriguez, S. *et al.* Titan's cloud seasonal activity from winter to spring with Cassini/VIMS. *Icarus* **216**, 89–110 (2011).
13. Mitchell, J. L., Ádámkóvics, M., Caballero, R. & Turtle, E. P. Locally enhanced precipitation organized by planetary-scale waves on Titan. *Nature Geosci.* **4**, 589–592 (2011).
14. Schneider, T., Graves, S. D. B., Schaller, E. L. & Brown, M. E. Polar methane accumulation and rainstorms on Titan from simulations of the methane cycle. *Nature* **481**, 58–61 (2012).
15. Turtle, E. P. *et al.* Seasonal changes in Titan's meteorology. *Geophys. Res. Lett.* **38**, L03203 (2011).
16. Turtle, E. P. *et al.* Rapid and extensive surface changes near Titan's equator: Evidence of April showers. *Science* **331**, 1414–1417 (2011).
17. Griffith, C. A. *et al.* Characterization of clouds in Titan's tropical atmosphere. *Astrophys. J.* **702**, L105–L109 (2009).
18. Mahoney, K. M., Lackmann, G. M. & Parker, M. D. The role of momentum transport in the motion of a quasi-idealized mesoscale convective system. *Mon. Weath. Rev.* **137**, 3316–3338 (2009).
19. Fulchignoni, M. *et al.* *In situ* measurements of the physical characteristics of Titan's environment. *Nature* **438**, 1–7 (2005).
20. Niemann, H. B. *et al.* The abundances of constituents of Titan's atmosphere from the GCMS instrument on the Huygens probe. *Nature* **438**, 1–6 (2005).
21. Lorenz, R. D. Physics of saltation and sand transport on Titan: A brief review. *Icarus* **230**, 162–167 (2014).
22. Bridges, N. T. *et al.* Earth-like sand fluxes on Mars. *Nature* **485**, 339–342 (2012).
23. Burr, D. M. *et al.* Higher-than-predicted saltation threshold wind speeds on Titan. *Nature* **517**, 60–63 (2015).
24. Rubin, D. M. & Hunter, R. Bedform alignment in directionally varying flows. *Science* **237**, 276–278 (1987).
25. Courrech du Pont, S., Narteau, C. & Gao, X. Two modes for dune orientation. *Geology* **42**, 743–746 (2014).
26. Rubin, D. M. & Hesp, P. A. Multiple origins of linear dunes on Earth and Titan. *Nature Geosci.* **2**, 653–658 (2009).
27. Radebaugh, J. *et al.* Dunes on Titan observed by Cassini Radar. *Icarus* **194**, 690–703 (2008).
28. Ewing, R. C., Hayes, A. G. & Lucas, A. Sand dune patterns on Titan controlled by long-term climate cycles. *Nature Geosci.* **8**, 15–19 (2015).
29. Lucas, A. *et al.* Growth mechanisms and dune orientation on Titan. *Geophys. Res. Lett.* **41**, 6093–6100 (2014).
30. Miller, S. *et al.* Haboob dust storms of the southern Arabian Peninsula. *J. Geophys. Res.* **113**, D01202 (2008).

### Acknowledgements

We thank J.-Y. Grandpeix, F. Forget, A. Spiga and J. Leconte for helpful discussions. We acknowledge financial support from the UnivEarthS LabEx program of Sorbonne Paris Cité (ANR-10-LABX-0023 and ANR-11-IDEX-0005-02), the French National Research Agency (ANR-12-BS05-001-03/EXO-DUNES) and the Centre National d'Etudes Spatiales. B.C. acknowledges support from an appointment to the NASA Postdoctoral Program at NAI Virtual Planetary Laboratory, administered by Oak Ridge Affiliated Universities.

### Author contributions

B.C. developed the idea of the methane storm control. E.B. and S.R. developed and ran the mesoscale model. S.L. and B.C. developed and ran the GCM. B.C. analysed the simulations. C.N. and S.C.P. provided the dune growth mechanism and Fig. 4b. A.L. provided the denoised image and orientations of Titan's dunes. B.C. wrote the paper with significant contributions from all the authors in interpreting the results and editing of the manuscript.

### Additional information

Supplementary information is available in the [online version of the paper](#). Reprints and permissions information is available online at [www.nature.com/reprints](http://www.nature.com/reprints). Correspondence and requests for materials should be addressed to B.C.

### Competing financial interests

The authors declare no competing financial interests.